Scientific Research Publishing

Int. J. Communications, Network and System Sciences, 2022, 15, 79-93
https://www.scirp.org/journal/ijcns
ISSN Online: 1913-3723
ISSN Print: 1913-3715

Model Predictive Direct Torque Control of Permanent Magnet Synchronous Motor (PMSM) with Online Parameter Estimation Based on Extended Kalman Filter

Gang Yang[1,2], Xiao Jiang[3], Shuaishuai Lv[3]

[1]First Institute of Oceanography, Ministry of Natural Resources, Qingdao, China
[2]Pilot National Laboratory for Marine Science and Technology (Qingdao), Qingdao, China
[3]School of Electronics and Information, Hangzhou Dianzi University, Hangzhou, China
Email: yanggang@fio.org.cn, jx@hdu.edu.cn, lvshuai@hdu.edu.cn

How to cite this paper: Yang, G., Jiang, X. and Lv, S.S. (2022) Model Predictive Direct Torque Control of Permanent Magnet Synchronous Motor (PMSM) with Online Parameter Estimation Based on Extended Kalman Filter. *Int. J. Communications, Network and System Sciences*, **15**, 79-93.
https://doi.org/10.4236/ijcns.2022.157007

Received: March 29, 2022
Accepted: July 22, 2022
Published: July 25, 2022

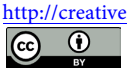

Abstract

Aiming at the torque and flux ripples in the direct torque control and the time-varying parameters for permanent magnet synchronous motor (PMSM), a model predictive direct torque control with online parameter estimation based on the extended Kalman filter for PMSM is designed. By predicting the errors of torque and flux based on the model and the current states of the system, the optimal voltage vector is selected to minimize the error of torque and flux. The stator resistance and inductance are estimated online via EKF to reduce the effect of model error and the current estimation can reduce the error caused by measurement noise. The stability of the EKF is proved in theory. The simulation experiment results show the method can estimate the motor parameters, reduce the torque, and flux ripples and improve the performance of direct torque control for permanent magnet synchronous motor (PMSM).

Keywords

Model Predictive Direct Torque Control, Extended Kalman Filter, Parameter Estimation, Permanent Magnet Synchronous Motor, Filter's Stability

1. Introduction

In the traditional direct torque control (DTC) method of permanent magnet synchronous motor (PMSM), the adjustment of the torque and flux by the hysteresis comparator is of Bang-Bang control, and the voltage vector is chosen by

table lookup according to different sectors, so the deviation size cannot be distinguished [1]; The pure integral method is mostly used for traditional DTC flux observation, greatly affected by motor parameters, causing inaccurate flux and torque estimation and large torque and flux ripples [2] [3].

To overcome the disadvantages of traditional DTC, and improve the control performance of traditional DTC, the hysteresis comparator is improved (such as control method [4] combining the space vector modulation (SVM) technology and the traditional DTC) so that SVM-DTC can obtain continuously changing space voltage vector to achieve accurate control of torque and flux. The literature [5] subdivides traditional 6 sectors into 18 sectors by the technology of combining the sector subdivision and the duty cycle, and calculates and adjusts the action time of effective voltage vector promptly according to torque error to reduce the torque ripple. Furthermore, the torque and flux observation accuracy directly determine the performance of DTC, thus improving the stator flux and torque observation accuracy is another way to reduce the torque ripple. To improve the observation accuracy of flux and torque, the full order observer, nonlinear feedback correction compensation observer, sliding-mode observer [6] [7] [8], etc. are used for PMSM-DTC control system.

The model predictive control (MPC) is also called as receding horizon control and a feedback control strategy widely discussed in recent years. The basic principle of MPC is to use the model of the system to predict and optimize the future behavior of the system. By combining MPC with traditional DTC, the literature [9] proposes the DTC control (MPDTC) based on MPC for induction motor, and uses the cost function to replace the hysteresis comparator of traditional DTC pursuant to the predicted torque and flux error to seek for the space voltage vector that minimizes the torque and flux among 8 space voltage vectors; The literature [10] combines MPDTC with duty cycle to reduce the torque and flux ripple. However, the PMSM model which is a time-varying model hasn't been considered in the above literature, and the accuracy of prediction model directly influences the torque control performance.

The extended Kalman filter (EKF) has an excellent state estimation capability for nonlinear systems, and can still estimate the state of the system especially in the case of noise and measurement bias errors [11]. EKF is widely used in the motor position less control system. The literature [12] [13] has adopted the stator flux, motor speed and rotor position, and designed the permanent magnet synchronous motor position less DTC control system. The literature [14] uses the EKF on-line estimation stator resistance and inductance for the maximum torque per ampere (MTPA) control system.

By combining the permanent magnet synchronous motor MPDTC and EKF online parameter estimation, this paper carries out online estimate of PMSM stator resistance and inductance parameters for the calibration of prediction model in MPDTC control. At the same time, EKF estimates the current of PMSM in a rotating coordinate system to correct the noise and bias errors when current sensor measurement. Therefore, the MPDTC of permanent magnet

synchronous motor based on EKF can overcome the torque ripple arising from traditional DTC hysteresis, and reduce the influence of motor parameter variation and measurement error on control accuracy. The simulation and experimental results show that the model predictive direct torque control for permanent magnet synchronous motor (PMSM) based on extended Kalman filter proposed in this paper can effectively reduce torque ripple, and is of good torque and flux control performance.

2. Model Predictive Direct Torque Control of the Permanent Magnet Synchronous Motor (PMSM)

2.1. Model of the Permanent Magnet Synchronous Motor (PMSM)

The voltage equation of permanent magnet synchronous motor in the rotating coordinate system is

$$\begin{cases} \dfrac{\mathrm{d}i_d}{\mathrm{d}t} = \dfrac{1}{L_d}\left(u_d - R_s i_d + \omega_e L_q i_q\right) \\ \dfrac{\mathrm{d}i_q}{\mathrm{d}t} = \dfrac{1}{L_q}\left(u_q - R_s i_q - \omega_e L_d i_d - \omega_e \varphi_f\right) \end{cases} \tag{1}$$

where i_d and i_q refer to direct-axis and cross-axis current; u_d and u_q refer to direct-axis and cross-axis voltage; R_s refers to stator resistance; L_d and L_q refer to direct-axis and cross-axis inductance. As for the surface-mount technology PMSM, $L_d = L_q = L_s$ and φ_f refer to rotor permanent magnet flux, and ω_e refers to rotor electric angle speed.

If the current in Equation (1) is in the state variable, namely $\boldsymbol{x} = \begin{bmatrix} i_d & i_q \end{bmatrix}^{\mathrm{T}}$, $\boldsymbol{u} = \begin{bmatrix} u_d & u_q & \varphi_f \end{bmatrix}^{\mathrm{T}}$, Equation (1) can be written as:

$$\dot{\boldsymbol{x}} = A\boldsymbol{x} + B\boldsymbol{u} \tag{2}$$

where $A = \begin{bmatrix} \dfrac{-R_s}{L_d} & \omega_e \\ -\omega_e & \dfrac{-R_s}{L_q} \end{bmatrix}$, $B = \begin{bmatrix} \dfrac{1}{L_d} & 0 & 0 \\ 0 & \dfrac{1}{L_q} & \dfrac{-\omega_e}{L_q} \end{bmatrix}$.

According to the literature [15], the prediction model of permanent magnet synchronous motor can be obtained by discretization of the model as follows:

$$\boldsymbol{x}(k+1) = \boldsymbol{F}(k)\boldsymbol{x}(k) + \boldsymbol{G}u(k) \tag{3}$$

where $\boldsymbol{x}(k) = \begin{bmatrix} i_d(k) & i_q(k) \end{bmatrix}^{\mathrm{T}}$, $\boldsymbol{u}(k) = \begin{bmatrix} u_d(k) & u_q(k) & \varphi_f \end{bmatrix}$

$$\boldsymbol{F}(k) = \begin{bmatrix} 1 - \dfrac{T_s R_s}{L_d} & T_s \omega_e(k) \\ -T_s \omega_e(k) & 1 - \dfrac{T_s R_s}{L_d} \end{bmatrix}, \quad B = \begin{bmatrix} \dfrac{T_s}{L_d} & 0 & 0 \\ 0 & \dfrac{T_s}{L_q} & \dfrac{-T_s \omega_e(k)}{L_q} \end{bmatrix}.$$

The corresponding motor flux and torque are:

$$\begin{cases} \varphi_d(k) = L_d i_d(k) + \varphi_f \\ \varphi_q(k) = L_q i_q(k) \end{cases} \tag{4}$$

$$\begin{cases} T_e(k) = \dfrac{3}{2} n_p \varphi_f i_q(k) \\ \varphi_s(k) = \sqrt{\varphi_d(k)^2 + \varphi_q(k)^2} \end{cases} \tag{5}$$

where $\varphi_d(k)$, $\varphi_q(k)$ refers to direct-axis and cross-axis flux at *k*, and $T_e(k)$, $\varphi_s(k)$ refers to electromagnetic torque and stator flux amplitude at *k*.

2.2. Model Predictive Direct Torque Control

The idea of model predictive direct torque control is to predict the flux and torque errors in the next control cycle according to the current torque, flux state and voltage vector in the discrete state, and select the voltage vector minimizing the cost function from the eight voltage vectors pursuant to the cost function chosen. The Control Block Diagram of MPDTC is shown in Figure 1.

The realization process for MPDTC of permanent magnet synchronous motor can be divided into several parts below:

1) Measurement: The stator current, rotor position and stator voltage of the current control cycle can be measured by the corresponding sensor, and the rotation rate can be calculated by position differential;

2) Prediction: Bring the current stator current and speed into Equation (3), and calculate the predicted values of electromagnetic torque and flux linkage corresponding to 8 inverter switching states after one cycle as per (4)-(5);

3) Evaluation: Calculate the corresponding evaluation function values by the predicted and given values of torque and flux obtained based on different voltage vectors, and select the voltage vector corresponding to the minimum evaluation function;

4) Implementation: Apply the chosen optimal voltage vector to the inverter to drive the permanent magnet synchronous motor.

The most important indicators of MPDTC control performance are the torque and flux error values. Set the evaluation function *J* in Equation (6) to minimize torque and flux errors:

$$J = \lambda_T \left| T_e^* - T_e(k+1) \right|^2 + \lambda_\varphi \left\| \varphi_s^* \right| - \left| \varphi_s(k+1) \right\|^2 \tag{6}$$

where λ_T and λ_φ refer to weight coefficient, respectively.

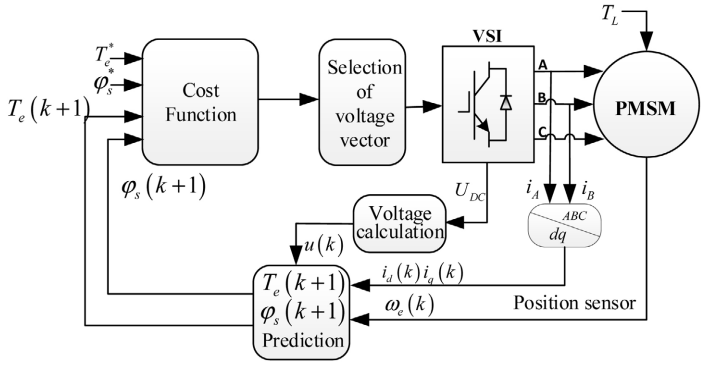

Figure 1. The control block diagram for MPDTC.

3. Parameter Estimation Based on Extended Kalman Filter (EKF)

3.1. Model of Parameter Estimation Based on Extended Kalman Filter

According to Equation (1), the equation of state when the parameters are time-varying can be obtained as follows:

$$\begin{cases} \dot{\boldsymbol{x}}(t) = f\left(\boldsymbol{x}(t), u(t)\right) + \sigma(t) \\ \boldsymbol{y} = H\boldsymbol{x}(t) + \mu(t) \end{cases} \tag{7}$$

where $\sigma(t)$ refers to motor parameter change and other system noise; $\mu(t)$ refers to noise arising from the system, $\boldsymbol{x} = \begin{bmatrix} i_d & i_q & a & b \end{bmatrix}^{\mathrm{T}}$, $a = 1/L_s$, $b = R_s$, $f\left(\boldsymbol{x}(t)\right) = \begin{bmatrix} -abi_d + \omega_e i_q + au_d \\ -abi_q - \omega_e i_d - a\omega_e \varphi_f + u_q \\ 0 \\ 0 \end{bmatrix}$; $G = \begin{bmatrix} a & 0 \\ 0 & b \\ 0 & 0 \\ 0 & 0 \end{bmatrix}$; $H = I_{4\times 4}$.

If the optimal value of the state variable $x(t)$ estimated at t is $\hat{\boldsymbol{x}}$, the estimation error can be defined as:

$$\Delta\boldsymbol{x} = \boldsymbol{x} - \hat{\boldsymbol{x}} \tag{8}$$

Expand $f\left(\boldsymbol{x}(t)\right)$ at $\hat{\boldsymbol{x}}$ as a Taylor series, ignore higher-order terms and consider Equation (8) to obtain:

$$\Delta\dot{\boldsymbol{x}} = F\Delta\boldsymbol{x} \tag{9}$$

where $F = \left.\dfrac{\partial f\left(\boldsymbol{x}(t)\right)}{\partial \boldsymbol{x}}\right|_{\boldsymbol{x}=\hat{\boldsymbol{x}}}$.

Set the sampling time to be T_s which is small enough, and discretize the above equation to obtain the discrete nonlinear system equation of Equation (7):

$$\begin{cases} \boldsymbol{x}(k+1) = F_{k+1,k}\boldsymbol{x}(k) + \tilde{\boldsymbol{u}}(k) + \sigma(k) \\ \boldsymbol{y}(k+1) = H\boldsymbol{x}(k+1) + \mu(k) \end{cases} \tag{10}$$

where $F_{k+1,k}$ refers to state transition matrix. When the sample time is small enough, $F_{k+1,k} \approx I + T_s \left.\dfrac{\partial f\left(\boldsymbol{x}(t)\right)}{\partial \boldsymbol{x}}\right|_{\boldsymbol{x}_k=\hat{\boldsymbol{x}}_k}$ exists, and I refers to unit matrix; Record $F_{k+1|k} = \left.\dfrac{\partial f\left(\boldsymbol{x}(t)\right)}{\partial \boldsymbol{x}}\right|_{\boldsymbol{x}_k=\hat{\boldsymbol{x}}_k}$ and $\tilde{\boldsymbol{u}}(k) = f\left(\hat{x}_{k|k}\right) - F_{k+1,k}\hat{x}_{k|k} + Gu(k)$.

3.2. Algorithm of Parameter Estimation Based on Extended Kalman Filter (EKF)

After discretization of PMSM nonlinear system, according to recursion formula of EKF, the recursion formula of parameter estimation of PMSM can be obtained as:

$$\hat{x}_{k|k-1} = \hat{x}_{k-1|k-1} + \left[f\left(\hat{x}_{k-1|k-1}\right) + G_{k-1}u_{k-1} \right] T_s \tag{11}$$

$$P_{k|k-1} = F_{k+1,k} P_{k-1} F_{k+1,k}^{\mathrm{T}} + Q \tag{12}$$

$$K_k = P_{k|k-1} H^{\mathrm{T}} \left(H P_{k|k-1} H^{\mathrm{T}} + R \right)^{-1} \tag{13}$$

$$P_{k|k} = \left(I - K_k H \right) P_{k|k-1} \tag{14}$$

$$\hat{x}_{k|k} = \hat{x}_{k|k-1} + K_k \left(y_k - H \hat{x}_{k|k-1} \right) \tag{15}$$

wherein, $P_{k|k-1}$ refers to error covariance matrix, $\hat{x}_{k|k-1}$ refers to state prediction vector, $P_{k|k}$ refers to updated covariance matrix, K_k refers to updated filter gain matrix, y_k refers to measured value and $\hat{x}_{k|k}$ refers to optimum estimate.

To simplify the calculation, the state transition matrix $F_{k+1,k}$ in Equation (12) is replaced by $F_{k+1|k}$, and the infinite minor term of T_s^2 is ignored to simplify Equation (12) as:

$$P_{k|k-1} = P_{k-1|k-1} + \left(F_{k-1|k-1} P_{k-1|k-1} + P_{k-1|k-1} F_{k-1|k-1}^{\mathrm{T}} \right) T_s + Q \tag{16}$$

According to Equations (11)-(16), the steps of the Kalman filter can be obtained as follows:

1) Prediction update: As per the input and the best value of the last estimate, the state estimate value of the latest step can be obtained by bringing into Equation (10);

2) Update of error covariance matrix and gain matrix. Update the error covariance matrix and filter gain matrix in accordance with Equations (12), (13) and (14);

3) Update of optimum estimate. Estimate the optimal value of the current state (namely Equation (15)) pursuant to current measured value and current estimate value.

4) In line with the estimated optimal current and PMSM motor parameters, the optimal electromagnetic torque and flux can be estimated by bringing into Equation (5), and the motor parameters shall be updated in the predictive control algorithm.

$$\begin{cases} \hat{T}_e(k) = \dfrac{3}{2} n_p \varphi_f \hat{i}_q(k) \\ \hat{\varphi}_s(k) = \sqrt{\hat{\varphi}_d(k)^2 + \hat{\varphi}_q(k)^2} \end{cases} \tag{17}$$

4. Analysis of Stability

The MPDTC system of PMSM is a typical nonlinear system and its stability consists of two parts: Firstly, stability of the original system; Secondly, stability of designed EKF. According to literature [16], the EKF of the uniformly completely controllable and observable system is stable, and the initial value of the error covariance matrix can be arbitrary value.

Pursuant to Equations (10)-(15), the equation of discrete EKF can be obtained as follows:

$$\hat{x}_{k+1|k+1} = P_{k+1|k+1}P_{k+1|k}^{-1}F_{k+1,k}\hat{x}_{k|k} + \tilde{z}_{k+1} \tag{18}$$

where $\tilde{z}_{k+1} = K_{k+1}\left(y_{k+1} - H\tilde{u}_k\right) + \tilde{u}_k$ is the irrelative term of Equation and $\hat{x}_{k|k}$, and can be seen as input, and $P_{k+1|k+1}P_{k+1|k}^{-1}F_{k+1,k}$ refers to transition matrix. In case of making $M_{k+1} = \hat{x}_{k+1|k+1}$, the homogeneous equation corresponding to Equation (18) is

$$M_{k+1} = P_{k+1|k+1}P_{k+1|k}^{-1}F_{k+1,k}M_k \tag{19}$$

To prove the convergence of EKF, three assumptions and one lemma are put forward:

Assumption 1: The original system is uniformly completely controllable and observable. As per the state equation and output equation of the system, the system is obviously a controllable and observable system and a physically realizable system that is to say that the system is a bounded input and output system, so the assumption is established.

Assumption 2: If the system is uniformly completely controllable and observable, the EKF error variance matrix $P_{k|k}$ will be with upper bound and lower bound, namely existence of positive integer-N and $\overline{p} > 0$ $\underline{p} > 0$) (unrelated to $\underline{p}$ and k) to realize for each $k > N$:

$$\underline{p}I \le P_{k|k} \le \overline{p}I \tag{20}$$

Assumption 3: Further assume that $\left\|F_{k|k-1}\right\|$, $\|H\|$ is positive, $\overline{f}$, $\underline{f}$ and $\overline{h}$, $\underline{h}$ for any upper bound and lower bound, while the zero-mean white noise is bounded, and its upper bound and lower bound are set as $\overline{q}$, $\underline{q}$ and $\overline{r}$, $\underline{r}$.

Lemma 1: As for the invertible matrix A, C and G, if $I + C\left(sI - A\right)^{-1}G$ is reversible, the $I + C\left(sI - A\right)^{-1}G$ inverse matrix is:

$$\left[I + C\left(sI - A\right)^{-1}G\right]^{-1} = I - C\left(sI - A + GC\right)^{-1}G \tag{21}$$

Proof: In case of noting $B = sI - A$,

$$\begin{aligned}
&\left(I - C\left(B + GC\right)^{-1}G\right)\left(I + CB^{-1}G\right)\\
&= I + CB^{-1}G - C\left(B + GC\right)^{-1}G - C\left(B + GC\right)^{-1}GCB^{-1}G\\
&= I + CB^{-1}G - C\left(\left(B + GC\right)^{-1} - \left(B + GC\right)^{-1}GCB^{-1}\right)G\\
&= I + CB^{-1}G - C\left(\left(B + GC\right)^{-1}\left(I - GCB^{-1}\right)\right)G\\
&= I + CB^{-1}G - C\left(\left(B + GC\right)^{-1}\left(BB^{-1} - GCB^{-1}\right)\right)G\\
&= I + CB^{-1}G - C\left(\left(B + GC\right)^{-1}\left(\left(B - GC\right)B^{-1}\right)\right)G\\
&= I + CB^{-1}G - CB^{-1}G = I
\end{aligned}$$

The authentication is over.

Theorem 1: Under three assumptions, if there is a Lyapunov function-$V_p\left[M_k, k\right]$, and $V_p\left[0, k\right] \equiv 0$, the system (19) is of uniform asymptotic stability within a large scope, that is to say that the system (18) is also a uniformly asymptotically stable system within a large scope.

Proof: Select a scalar function:

$$V_p\left[M_k,k\right]=M_k^{\mathrm{T}}P_{k|k}^{-1}M_k \tag{22}$$

In case of $\underline{p}I\le P_{k|k}\le \overline{p}I$ as per Assumption 1 and 2, $\frac{1}{\overline{p}}I\le P_{k|k}\le \frac{1}{\underline{p}}I$ will be established. In case of multiplying by M_k^{T} and M_k on the left and on the right, respectively, can be obtained,

$$M_k^{\mathrm{T}}\frac{1}{\overline{p}}M_k\le M_k^{\mathrm{T}}P_{k|k}M_k\le M_k^{\mathrm{T}}\frac{1}{\underline{p}}M_k$$

The above can be rewritten as:

$$\frac{1}{\overline{p}}\left\|M_k\right\|^2\le V_p\left[M_k,k\right]\le\frac{1}{\underline{p}}\left\|M_k\right\|^2 \tag{23}$$

Set $\alpha_1=\frac{1}{\overline{p}}\left\|M_k\right\|^2$, $\alpha_2=\frac{1}{\underline{p}}\left\|M_k\right\|^2$, α_1, α_2 is the nondecreasing scalar function related to $\left\|M_k\right\|^2$ with

$$\begin{cases}\alpha_2>\alpha_1\ge 0\\ \alpha_1\le V_p\left[M_k,k\right]\le\alpha_2\\ M_k\ne 0\end{cases} \tag{24}$$

The function $V_p\left[M_k,k\right]$ is a bounded function;

Pursuant to Equation (12), upon inversion, obtain

$$P_{k+1|k}^{-1}=\left(F_{k+1,k}P_{k|k}F_{k+1,k}^{\mathrm{T}}+Q\right)^{-1} \tag{25}$$

In case of multiplying Equation (25) above by $F_{k+1,k}^{\mathrm{T}}$ and $F_{k+1,k}$ on the left and on the right, respectively, obtain

$$\begin{aligned}F_{k+1,k}^{\mathrm{T}}P_{k+1|k}^{-1}F_{k+1,k}&=F_{k+1,k}^{\mathrm{T}}\left(F_{k+1,k}P_{k|k}F_{k+1,k}^{\mathrm{T}}+Q\right)^{-1}F_{k+1,k}\\&=\left(P_{k|k}+F_{k+1,k}^{-1}QF_{k+1,k}^{-\mathrm{T}}\right)^{-1}\end{aligned} \tag{26}$$

As per Lemma 1, Equation (26) can be expressed as:

$$F_{k+1,k}^{\mathrm{T}}P_{k+1|k}^{-1}F_{k+1,k}=P_{k|k}^{-1}-P_{k|k}^{-1}\left(P_{k|k}^{-1}+F_{k+1,k}Q^{-1}F_{k+1,k}^{\mathrm{T}}\right)^{-1}P_{k|k}^{-1} \tag{27}$$

Based on Equation (19) and (22), obtain

$$V_{p+1}\left[M_{k+1},k+1\right]=M_{k+1}^{\mathrm{T}}P_{k+1|k+1}^{-1}M_{k+1}=M_k^{\mathrm{T}}F_{k+1,k}^{\mathrm{T}}P_{k+1|k}^{-\mathrm{T}}P_{k+1|k+1}^{\mathrm{T}}P_{k+1|k+1}^{-1}P_{k+1|k}^{-1}F_{k+1,k}M_k \tag{28}$$

Pursuant to Equation (14), $P_{k+1|k+1}=\left(I-K_{k+1}H\right)P_{k+1|k}$ can be deduced, and $P_{k+1|k+1}^{\mathrm{T}}=P_{k+1|k}^{\mathrm{T}}\left(I-K_{k+1}H\right)^{\mathrm{T}}$ can be obtained. In case of bringing in Equation (28), obtain

$$\begin{aligned}&V_{p+1}\left[M_{k+1},k+1\right]\\&=M_k^{\mathrm{T}}F_{k+1,k}^{\mathrm{T}}P_{k+1|k}^{-1}F_{k+1,k}M_k-M_k^{\mathrm{T}}F_{k+1,k}^{\mathrm{T}}\left(K_{k+1}H\right)^{\mathrm{T}}P_{k+1|k}^{-1}F_{k+1,k}M_k\end{aligned} \tag{29}$$

After bringing Equation (27) into Equation (29), get

$$V_{p+1}\left[M_{k+1},k+1\right]=V_p\left[M_k,k\right]-M_k^{\mathrm{T}}P_{k|k}^{-1}\left(P_{k|k}^{-1}+F_{k+1,k}Q^{-1}F_{k+1,k}^{\mathrm{T}}\right)^{-1}P_{k|k}^{-1}M_k^{\mathrm{T}} \\ -M_k^{\mathrm{T}}F_{k+1,k}^{\mathrm{T}}\left(K_{k+1}H\right)^{\mathrm{T}}P_{k+1|k}^{-1}F_{k+1,k}M_k \tag{30}$$

Also pursuant to Equation (13), obtain

$$K_{k+1}H=P_{k+1|k}\left(P_{k+1|k}H^{\mathrm{T}}+H^{-1}RH^{-1}\right)^{-1} \tag{31}$$

Upon bringing Equation (31) into Equation (30), after arrangement, obtain

$$V_{p+1}\left[M_{k+1},k+1\right]-V_p\left[M_k,k\right] \\ =-M_k^{\mathrm{T}}\left(P_{k|k}+P_{k|k}F_{k+1,k}^{\mathrm{T}}Q^{-1}F_{k+1,k}^{\mathrm{T}}P_{k|k}\right)^{-1}M_k^{\mathrm{T}} \\ -M_k^{\mathrm{T}}\left(F_{k+1,k}^{-1}P_{k+1|k}F_{k+1,k}^{-\mathrm{T}}+F_{k+1,k}^{-1}P_{k+1|k}H^{-1}RH^{-\mathrm{T}}P_{k+1|k}^{-1}F_{k+1,k}^{-\mathrm{T}}\right)^{-1}M_k \tag{32}$$

Because of $P_{k|k}+P_{k|k}F_{k+1,k}^{\mathrm{T}}Q^{-1}F_{k+1,k}^{\mathrm{T}}P_{k|k}\le\overline{p}\left(1+\dfrac{\overline{p}\overline{f}^2}{\underline{q}}\right)=r_1$,

$F_{k+1,k}^{-1}P_{k+1|k}F_{k+1,k}^{-\mathrm{T}}+F_{k+1,k}^{-1}P_{k+1|k}H^{-1}RH^{-\mathrm{T}}P_{k+1|k}^{-1}F_{k+1,k}^{-\mathrm{T}}\le\dfrac{1}{\underline{f}^2}\left(\overline{p}+\dfrac{\overline{r}}{\underline{h}^2\underline{p}}\right)=r_2$, Equation (32) can be written as a discrete recursive inequality:

$$V_{p+1}\left[M_{k+1},k+1\right]-V_p\left[M_k,k\right]\le-\frac{\left\|M_k\right\|^2}{r_1r_2} \tag{33}$$

To sum up, the Lyapunov function $V_p\left[M_k,k\right]$ is bounded with monotone decreasing due to $r_1>0$, $r_2>0$, so the designed EKF is uniformly asymptotically stable, that is to say that EKF is of bounded output.

As for the whole system, the original system is of uniform asymptotic stability, and the EKF estimation system is uniformly asymptotically stable, so the whole system designed is also uniformly asymptotically stable.

5. Simulation Results

To verify the validity of the proposed method, the MATLAB/Simulink is used to establish the simulation model of the system. The Control Block Diagram is shown in Figure 2. The permanent magnet synchronous motor parameters are shown in Table 1.

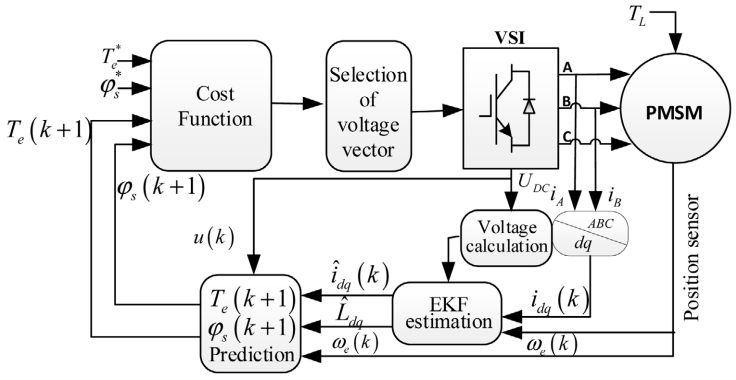

Figure 2. The control block diagram of MPDTC based on EKF.

Table 1. Motor parameters.

Parameter	Parameter description	Value
V_{DC} (V)	DC voltage	300
R (Ω)	Stator resistance	1.73
L_d, L_q (mH)	Stator inductance	8.5
φ_f (Wb)	Rotor magnet flux	0.0503
ω_n (rpm)	Rated speed	3000
T_n (Nm)	Rated torque	4.77
n_p	Number of pole pairs	5
J (kg·m^2)	Rotor inertia	0.0006
B	Friction coefficient	0.0003

The state estimation and parameter estimation module based on EKF is realized by S-Function. Theoretically, the covariance matrix of noise determines the convergence and stability of EKF with Q and R being $Q = diag[1,1,1,1]$ and $R = diag[1,1]$, respectively. The initial value of the error covariance matrix- P_0 can be selected randomly, but a diagonal matrix larger than that when EKF converges is generally chosen to improve the performance and convergence rate of EKF. $P_0 = diag[1,1,1,1]$ is chosen in this paper.

In the simulation process, the maximum switching frequency and sampling time are 10 KHz and 100 μs, respectively. To verify the accuracy of parameter estimation, the robustness of motor parameter estimation at different speeds is verified firstly. The estimation result is shown in **Figure 3**. The given initial resistance value is 0.5 time of actual resistance value, and the give inductance value is 2 times of actual inductance value. The simulation results show that the actual value has been tracked at 0.08s, the maximum steady-state error on tracking is 6.8%, and the resistance and inductance estimation results are little affected in the process of speed change.

Figure 4 is the torque and speed waveform when the measurement noise occurs to the current sensor. **Figure 4(a)** is the actual torque and speed signal after the interference signal with an average value of 0 added to the current. As per the figures, the torque signal is with obvious burrs, and the speed feedback signals are also influenced in case of interference in current measurement. **Figure 4(b)** shows the torque and current waveform after the current signal is filtered by EKF. Compared to **Figure 4(a)**, the waveform of torque and speed decreases significantly.

When the resistance and inductance change, the control parameters in the MPDTC contain resistance and inductance parameters causing the control effect is affected by the resistance and inductance. **Figure 5** and **Figure 6** show that the load torque is rated load and 0.5 time of rated load, respectively when the resistance and inductance are 0.6 time of actual value and 1.5 times of actual

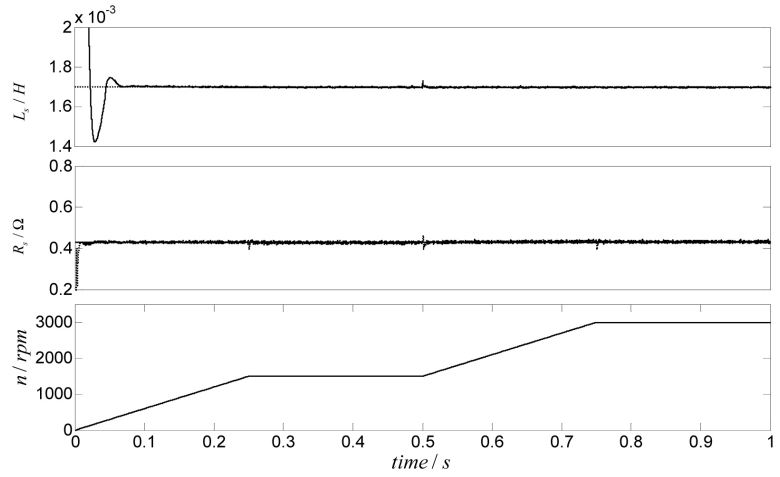

Figure 3. Parameter estimation based on different speeds and initial values.

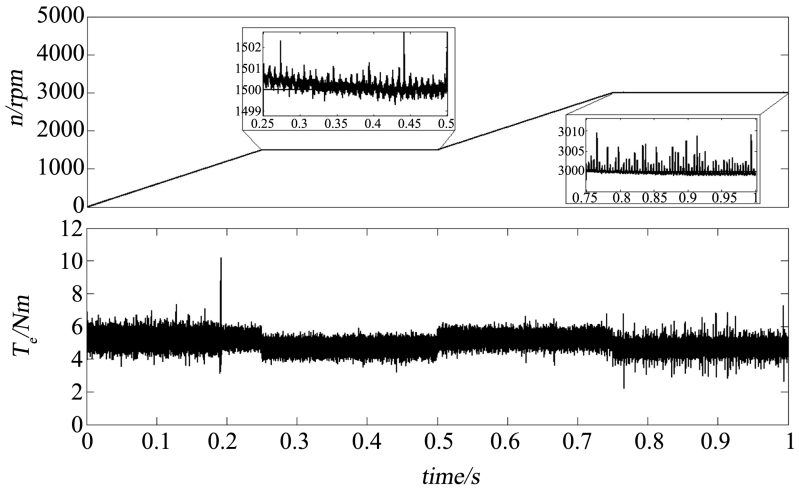

(a)

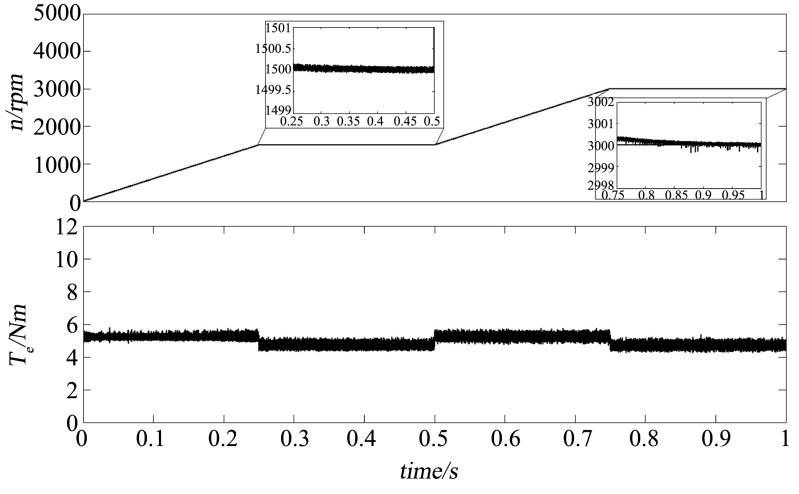

(b)

Figure 4. Current based on d_q coordinates in case of any interference. (a) Actual current based on d_q coordinates when the interference arises; (b) Actual current based on d_q coordinates after EKF filtering in case of any interference.

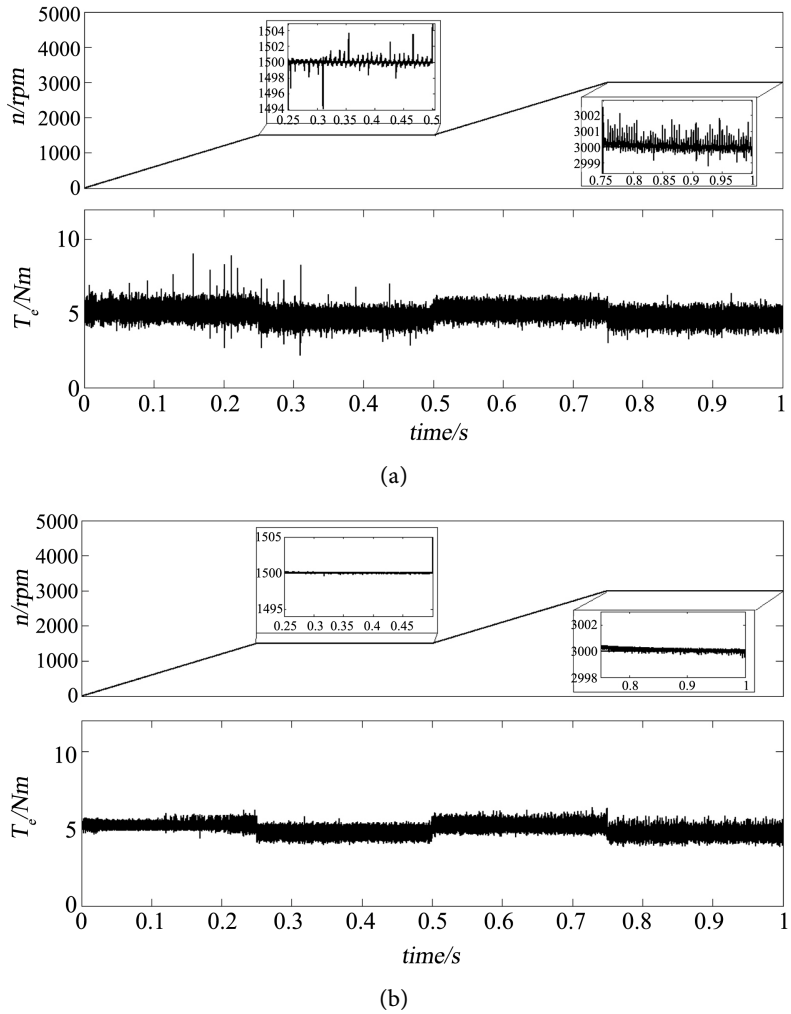

Figure 5. Speed and torque curve with parameter changing to 0.6 time.

value. The control effect of the controller before parameter adjustment is shown in **Figure 5(a)** and **Figure 6(a)**, and the control effect of the controller after parameter adjustment is shown in **Figure 6(b)** and **Figure 7(b)**. **Figure 6** shows the actual parameter is 0.6 time of the original value. According to **Figure 5(a)**, when the resistance and inductance decrease, the electromagnetic torque and flux prediction models are influenced by parameters, leading to inaccurate prediction of torque and flux, and torque ripple, but the parameters have less influence as the speed increases. **Figure 6** Simulation Result When the Parameter Changes To 1.5 Times. Similar to the motor parameter reduction, the torque control accuracy is also influenced, causing the torque ripple.

Figure 7 and **Figure 8** show the estimation results of parameters by EKF after changes of resistance and inductance parameters. According to such figures, EKF can accurately estimate the resistance and inductance changes. To make predictive controller control smoother, the resistance and inductance values estimated by EKF are subject to median and mean filtering every 500 points, and the filtered resistance and inductance values are used in the MPDTC controller.

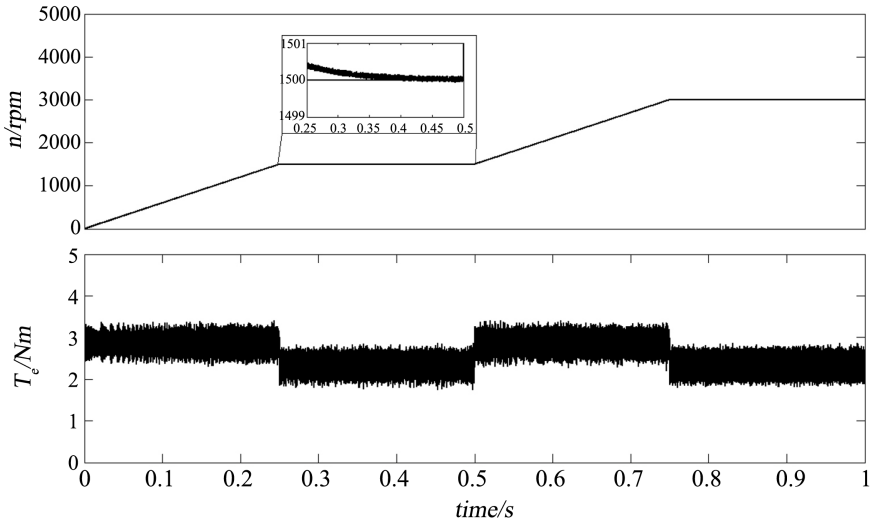

(a)

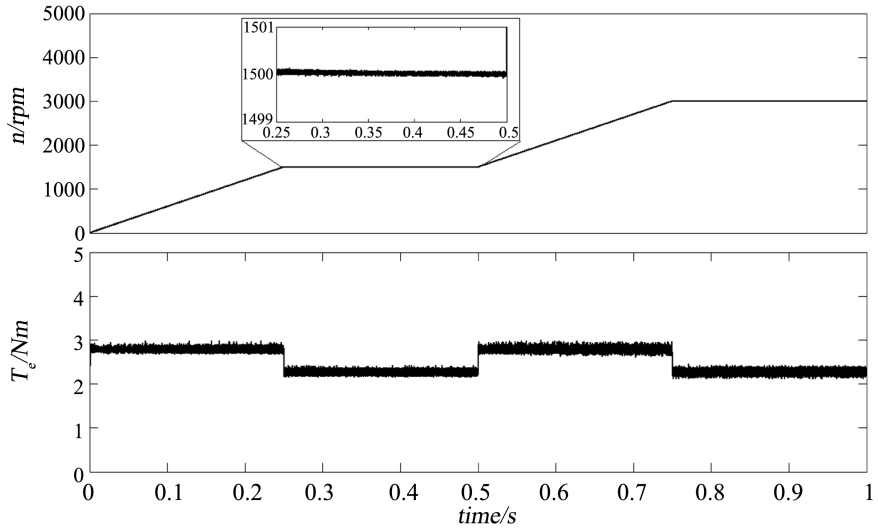

(b)

Figure 6. Speed and torque curve with parameter changing to 1.5 times.

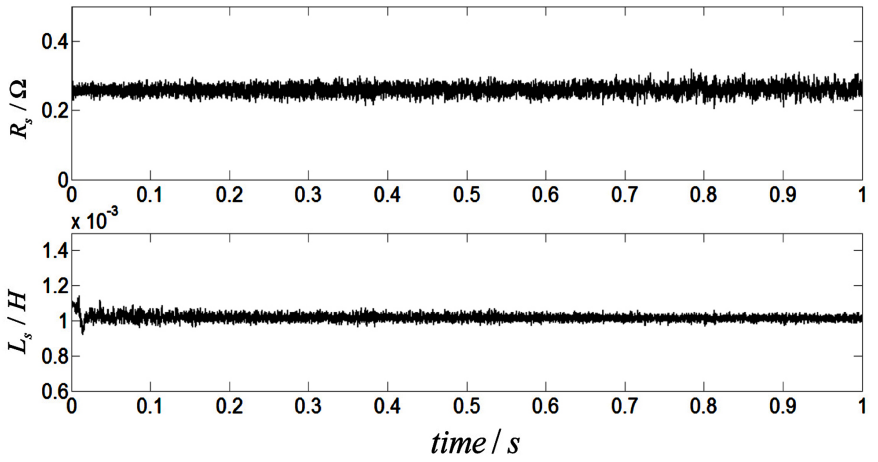

Figure 7. Estimation result with parameter changing to 0.6 time.

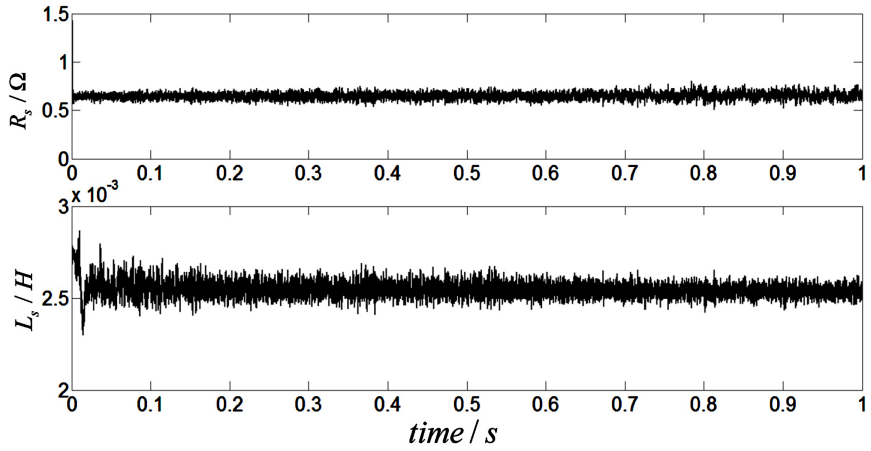

Figure 8. Estimation result with parameter changing to 1.5 times.

6. Conclusion

To suppress the torque and flux ripple of traditional direct torque control, this paper studies the model predictive direct torque control for permanent magnet synchronous motor (PMSM) based on EKF observer, seeks the optimal voltage vector which minimizes torque and flux among the 8 voltage vectors available pursuant to predicted torque error and flux error, carries out real-time estimation of resistance and inductance by the EKF observer, modifies the motor model parameters predicted by the model, and observes the direct-axis and cross-axis currents to compensate the torque and flux estimates and improve the calculation and estimation accuracy of torque and flux. The simulation results demonstrate the effectiveness of the method. In the future work, we can consider multi-step prediction and parameter time variation for further refinement.

Conflicts of Interest

The authors declare no conflicts of interest regarding the publication of this paper.

References

[1] Shi, C., Qiu, J. and Jin, M. (2005) Comparative Study on Direct Torque Control of Permanent Magnet Synchronous Motor. *Proceedings of the CSEE*, **25**, 141-146.

[2] Jia, H.P. and He, Y.K. (2006) Sliding Mode Variable Structure Direct Torque Control of Permanent Magnet Synchronous Motor. *Transactions of China Electrotechnical Society*, **21**, 1-6.

[3] Hariri, A.M., Aliabad, A.D., Ghafarzadeh, M. and Shamlou, S. (2020) Design, Analysis, and Fabrication of a Direct Drive Permanent NdFeB Magnet Synchronous Motor for Precision Position Control. *IET Electric Power Application*, **14**, 1438-1445. https://doi.org/10.1049/iet-epa.2018.5542

[4] Niu, F., Huang, X.Y. and Ge, L.J. (2019) A Simple and Practical Duty Cycle Modulated Direct Torque Control for Permanent Magnet Synchronous Motors. *IEEE Transactions on Power Electronics*, **34**, 1572-1579. https://doi.org/10.1109/TPEL.2018.2833488

[5] Xu, Y.P. and Zhong, Y.R. (2009) Direct Torque Control of Permanent Magnet Synchronous Motor Combining Sector Subdivision and Duty Ratio Control. *Proceedings of the CSEE*, **29**, 102-108.

[6] Liu, Y.H., Huo, H., Chu, B., *et al.* (2013) Passivity-Based Torque Tracking Control and Adaptive Observer Design of Inducstion Motors. *Control Theory and Applications*, **30**, 1021-1026.

[7] Zhuang, X. and Rahman, M.F. (2007) An Adaptive Sliding Stator Flux Observer for a Direct-Torque-Controlled IPM Synchronous Motor Drive. *IEEE Transactions on Industrial Electronics*, **54**, 2398-2406. https://doi.org/10.1109/TIE.2007.900328

[8] Liu, J., Chu, X.G. and Bai, H.Y. (2005) Study of Permanent Magnet Synchronous Motor Direct Torque Control Based on the Strategy of Reference Stator Flux Linkage and Voltage Space Vector Modulation. *Transactions of China Electrotechnical Society*, **2005**, 11-15.

[9] Geyer, T., Papafotiou, G. and Morari, M. (2009) Model Predictive Direct Torque Control-Part I: Concept, Algorithm, and Analysis. *IEEE Transactions on Industrial Electronics*, **56**, 1894-1905. https://doi.org/10.1109/TIE.2008.2007030

[10] Morel, F., Lin-Shi, X.F., Retif, J., Allard, B. and Buttay, C. (2009) A Comparative Study of Predictive Current Control Schemes for a Permanent-Magnet Synchronous Machine Drive. *IEEE Transactions on Industrial Electronics*, **56**, 2715-2728. https://doi.org/10.1109/TIE.2009.2018429

[11] Zhang, M., Xiao, X. and Li, Y.-D. (2007) Speed and Flux Observer of Permanent Magnet Synchronous Motor Based on Extended Kalman Filter. *Proceedings of the CSEE*, **27**, 36-40.

[12] Shi, K.L., Chan, T.F., Wong, Y.K. and Ho, S.L. (2002) Speed Estimation of an Induction Motor Drive Using an Optimized Extended Kalman Filter. *IEEE Transactions on Industrial Electronics*, **49**, 124-133. https://doi.org/10.1109/41.982256

[13] Bolognani, S., Tubiana, L. and Zigliotto, M. (2003) Extended Kalman Filter Tuning in Sensorless PMSM Drives. *IEEE Transactions on Industry Applications*, **39**, 1741-1747. https://doi.org/10.1109/TIA.2003.818991

[14] Sim, H.W., Lee, J. and Lee, K. (2014) On-line Parameter Estimation of Interior Permanent Magnet Synchronous Motor Using an Extended Kalman Filter. *Journal of Electrical Engineering & Technology*, **9**, 600-608. https://doi.org/10.5370/JEET.2014.9.2.600

[15] Fan, M.D., Lin, H. and Lan, T.Y. (2014) Model Predictive Direct Torque Control for SPMSM with Load Angle Limitation. *Progress in Electromagnetics Research B*, **58**, 245-256. https://doi.org/10.2528/PIERB14021106

[16] Nair, D.S., Jagadanand, G. and George, S. (2021) Torque Estimation Using Kalman Filter and Extended Kalman Filter Algorithms for a Sensorless Direct Torque Controlled BLDC Motor Drive: A Comparative Study. *Journal of Electrical Engineering & Technology*, **16**, 2621-2634.